Nonlinear MDOF system characterization and identification using the Hilbert-Huang transform

G. Kerschen[(1)], **A.F. Vakakis**[(2)], **Y.S. Lee**[(3)], **D.M. McFarland**[(3)], **L.A. Bergman**[(3)]
(1) University of Liège, Aerospace and Mechanical Engineering Department, Belgium
(2) National Technical University of Athens, Division of Mechanics, Greece
(3) University of Illinois at Urbana-Champaign, Department of Aerospace Engineering, U.S.A.
E-mail: g.kerschen@ulg.ac.be; vakakis@central.ntua.gr; yslee4,dmmcf,lbergman@uiuc.edu

Abstract
The Hilbert transform is one of the most successful approaches to tracking the varying nature of vibration of a large class of nonlinear systems thanks to the extraction of backbone curves from experimental data. Because signals with multiple frequency components do not admit a well-behaved Hilbert transform, it is inherently limited to the analysis of single-degree-of-freedom systems. In this study, the joint application of the complexification-averaging method and the empirical mode decomposition enables us to develop a new technique, the slow-flow model identification method. Through numerical and experimental applications, we demonstrate that the proposed method is adequate for characterizing and identifying multi-degree-of-freedom nonlinear systems.

1 Introduction

Nonlinear dynamics has been studied for a relatively long time, but the first contributions to the identification of nonlinear structural models date back only to the 1970s. Since then, numerous methods have been developed because of the highly individualistic nature of nonlinear systems. A large number of these methods were targeted at single-degree-of-freedom (SDOF) systems, but significant progress in the identification of multi-degree-of-freedom (MDOF) lumped-parameter systems was realized during the last ten years. However, it is fair to say that there is no general analysis method that can be applied to all nonlinear systems in all instances. For a review of the literature on the subject, the reader is invited to consult the monograph [1] or the recent overview [2].

One of the most successful approaches to nonlinear system identification is the restoring force surface method, introduced in the late 1970s by Masri and Caughey [3]. The technique is appealing in its simplicity, the starting point being Newton's second law. Another attractive technique, which uses the Hilbert transform and the slow-flow dynamics for nonlinear system identification, dates back to the early 1990s. SDOF systems were first studied in the 'FREEVIB' method [4], and the generalization to 2DOF systems soon followed [5]. That procedure tracks the varying nature of vibration of a large class of nonlinear systems thanks to the extraction of backbone curves from experimental data. Because multicomponent signals do not admit a well-behaved Hilbert transform, the 'FREEVIB' method is best exploited for SDOF systems or for single-mode resonance of MDOF systems. Alternative approaches for slow-flow-based identification were developed, using, for instance, the wavelet [6] and Gabor [7] transforms.

Recognizing the limitation of the Hilbert transform for signals with multiple frequency components, Huang et al. introduced the Hilbert-Huang transform (HHT) in 1998 in [8]. It decomposes signals in terms of elemental components, termed intrinsic mode functions (IMFs), through what has been called the empirical mode decomposition (EMD). Its capability to analyze nonlinear and nonstationary data, utilized in several applications such as plasma diagnostics [9] and financial time series [10], makes it potentially superior to the

Fourier and wavelet transforms. This is discussed in detail in the monograph [11]. Several applications of the HHT to structural dynamics recently appeared, including damage detection [12], gearbox and roller bearings fault diagnosis [13], aeroelastic flight data analysis [14], and nonlinear vibration characterization [15]. Yang et al. also related the IMFs to the modal properties, providing a clear interpretation of the relationship of HHT to linear dynamics [16, 17]. However, a complete analytical foundation is still lacking in the presence of nonlinear effects.

As shown for the first time in [18], the lack of this fundamental understanding of the HHT in nonlinear structural dynamics can be addressed by linking its outcome to the slow-flow dynamics of the system. The slow-flow model is established by performing a partition between slow and fast dynamics using the complexification-averaging (CxA) technique, resulting in a reduced dynamical system described by slowly-varying amplitudes and phases. Moreover, these slowly-varying variables can be extracted directly from experimental measurements using the Hilbert transform coupled with the EMD. The comparison between experimental and analytical results forms the basis of a novel parameter estimation method, termed the slow-flow model identification (SFMI) method. The SFMI method can be viewed as an effective generalization of the FREEVIB approach to MDOF systems.

This paper is organized as follows. In the next section, the CxA method is briefly presented. In Section 3, the HHT and the concept of an IMF are introduced; their use for nonlinear signal characterization is also detailed. The intimate relation between the CxA method and the HHT, which forms the basis of the SFMI method, is discussed in Section 4. The SFMI method is then demonstrated using numerical and experimental application examples in Sections 5 and 6, respectively. Finally, the method's strengths as well as its limitations are outlined in the conclusions of Section 7.

2 Modeling the Slow Flow of Nonlinear Systems: The CxA Method

The slow-flow model of a nonlinear system is established by partitioning its response in terms of slow and fast components, assuming that such decomposition is possible. This is the case when the time series of the dynamics are composed of a number of well separated dominant frequency components, which can be regarded as the fast frequencies of the response; the slow dynamics then provide the slowly-varying modulations of the fast-frequency components. The resulting equations govern the slow-flow variables, namely amplitudes and phases, and describe a dynamical system which is a good approximation to the original system under certain assumptions [19].

There are important motivations for studying the slow flow. One of them is that the slowly-varying amplitudes and phases represent meaningful features of the response and offer a sharper and clearer characterization of the system dynamics than the original time series. One possible method for deriving the slow dynamics of structural systems is the classical method of averaging [19]. In this study, a variant of this technique, the CxA method [20], is considered. There are basically four steps in the method: (i) complexification of the equations of motion; (ii) partition of the dynamics into slow and fast components; (iii) averaging of the fast-varying terms; and (iv) extraction of the slow-flow variables from the averaged system.

To illustrate the method, a damped Duffing oscillator

$$\ddot{x} + c\dot{x} + kx + k_{nl}x^3 = 0 \quad \text{with} \;\; x(0) = X, \; \dot{x}(0) = 0 \tag{1}$$

is first treated. A complex change of variable, $\psi(t) = \dot{x}(t) + j\omega x(t)$, is performed, where ω is the frequency which best describes the system response. Equation (1) becomes

$$\dot{\psi} - j\omega\frac{\psi + \psi^*}{2} + c\frac{\psi + \psi^*}{2} + k\frac{\psi - \psi^*}{2j\omega} + k_{nl}\left(\frac{\psi - \psi^*}{2j\omega}\right)^3 = 0. \tag{2}$$

The dynamics $\psi(t) = \varphi(t)e^{j\omega t}$ is decomposed into slow, $\varphi(t)$, and fast, $e^{j\omega t}$, components such that the motion is approximated by a single frequency component with modulated amplitude and phase. By averaging

out the fast-frequency component $e^{j\omega t}$, equation (2) is transformed into

$$\dot{\varphi} + \frac{j\omega\varphi}{2} + \frac{c\varphi}{2} - \frac{jk\varphi}{2\omega} - \frac{3jk_{nl}}{8\omega^3}|\varphi|^2\varphi = 0. \tag{3}$$

Due to the averaging process, this complex-valued differential equation represents an approximation to the original dynamics. We then proceed to the extraction of envelope and phase variables by expressing the variable $\varphi(t)$ in polar form, $\varphi(t) = a(t)e^{j\beta(t)}$,

$$\dot{a} + ja\dot{\beta} + \frac{j\omega a}{2} + \frac{ca}{2} - \frac{jka}{2\omega} - \frac{3jk_{nl}a^3}{8\omega^3} = 0. \tag{4}$$

The real and imaginary parts of this equation are

$$\dot{a} + \frac{ca}{2} = 0,\ \dot{\beta} + \frac{\omega}{2} - \frac{k}{2\omega} - \frac{3k_{nl}a^2}{8\omega^3} = 0;\ a(0) = X\omega,\ \beta(0) = \frac{\pi}{2}, \tag{5}$$

respectively. Unlike equation (1), the equations describing the slow-flow dynamics may be solved analytically, giving

$$a(t) = X\omega e^{-ct/2} \quad \text{and} \quad \beta(t) = \frac{3k_{nl}X^2}{8\omega c}(1 - e^{-ct}) - \left(\frac{\omega}{2} - \frac{k}{2\omega}\right)t + \frac{\pi}{2}. \tag{6}$$

Therefore, equations (5) may be viewed as a set of approximate but simplified equations that govern the essential dynamics of the system. The system response predicted by the CxA method is, in final form,

$$x(t) = \frac{a(t)}{\omega}\sin\left[\omega t + \beta(t)\right], \tag{7}$$

which shows that the total phase variable is $\Phi = \omega t + \beta$.

Because the primary focus of this paper is on MDOF nonlinear system identification, a 2DOF system is now investigated with equations of motion given by

$$\begin{aligned} m_1\ddot{x} + c_1\dot{x} + c_{12}(\dot{x} - \dot{y}) + k_1x + k_{12}(x - y) &= 0, \\ m_2\ddot{y} + c_{12}(\dot{y} - \dot{x}) + c_2\dot{y} + k_2y + k_{12}(y - x) + k_{nl}y^3 &= 0. \end{aligned} \tag{8}$$

The system response should comprise two dominant fast components with frequencies ω_1 and ω_2. Four complex variables are therefore introduced in this case,

$$\psi_1 = \dot{x}_1 + j\omega_1x_1, \quad \psi_2 = \dot{x}_2 + j\omega_2x_2, \quad \psi_3 = \dot{y}_1 + j\omega_1y_1, \quad \psi_4 = \dot{y}_2 + j\omega_2y_2, \tag{9}$$

such that $x(t) = x_1(t) + x_2(t)$ and $y(t) = y_1(t) + y_2(t)$. By substituting this ansatz into (8), applying multiphase averaging [21] over the fast-frequency components and expressing the complex amplitudes in polar form, the slow-flow model is derived (see [22] for the detailed computations).

Figure 1 shows the comparison between the system response predicted by the CxA method and the response computed using numerical simulation of the original equations of motion (8) with $k_1 = k_2 = k_{12} = m_1 = m_2 = 1$, $k_{nl} = 2$, $c_1 = c_2 = 0.05$, $c_{12} = 0$ and zero initial conditions except for $x(0) = 1$. Because the nonlinear coefficient and the initial displacement are $O(1)$ quantities, this is a strongly nonlinear system. Satisfactory agreement between prediction and numerical simulation is observed throughout the responses of the two oscillators. The good predictive capability of the CxA method for strongly nonlinear systems was previously discussed in [23], despite the absence of proof of asymptotic validity [19].

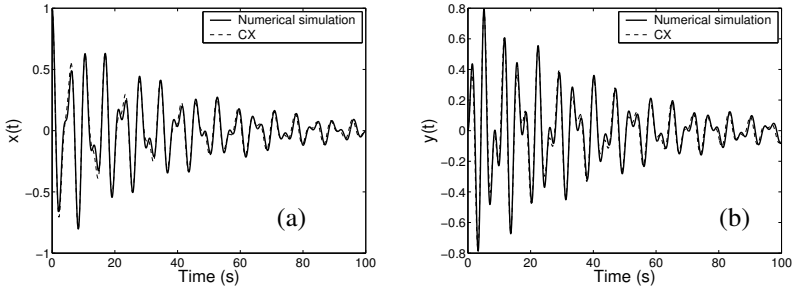

Figure 1: Approx. of the response of a 2DOF nonlinear system using the CxA method. (a) $x(t)$; (b) $y(t)$.

3 Characterization of a Multicomponent Signal: The HHT

The Hilbert transform of a time-domain signal $x(t)$ can be viewed as the convolution of the original signal with $1/t$, emphasizing temporal locality of $x(t)$. It characterizes the signal $x(t)$ through the extraction of its envelope $A(t)$ and instantaneous phase $\Phi(t)$, $x(t) = A(t)\cos\Phi(t)$. It is based on the analytic signal $X(t)$ defined as $X(t) = x(t) + jH[x(t)] = A(t)\exp[j\Phi(t)]$ where $j = \sqrt{-1}$ is the imaginary constant. Notice, at this point, the similarity of this complexification framework to the CxA process examined in the previous section. This is the first indication of the relationship between the two methods, which will be discussed in Section 4. It follows that

$$A(t) = \sqrt{x(t)^2 + H[x(t)]^2} \quad \text{and} \quad \Phi(t) = \arctan\left(H[x(t)]/x(t)\right). \tag{10}$$

The instantaneous frequency is the time derivative of the phase $\Phi(t)$. One intrinsic limitation of the method is that it is only truly suitable for monocomponent signals, i.e., those possessing a single dominant harmonic component.

The limitation of the Hilbert transform when applied to signals with multiple frequency components has been recently addressed through a process known as empirical mode decomposition (EMD) [8]. The basic idea of the EMD is to decompose the original signal in a sum of elemental components, termed intrinsic mode functions (IMFs). To be amenable to the Hilbert transform, each IMF must satisfy two properties: (i) the number of extrema and zero-crossings can differ by no more than one; and (ii) at any point, the mean value of the envelope defined by the local maxima and the envelope defined by the local minima should be zero. It follows that an IMF is a monochromatic signal, the amplitude and frequency of which can be modulated, unlike harmonic functions. Moreover, the signal can be reconstructed as a linear superposition of its IMFs. Taken collectively, the Hilbert spectra of the IMFs give a complete characterization of a multicomponent signal in terms of amplitude and phase variables, or equivalently in terms of amplitudes and instantaneous frequencies. The approach coupling the EMD with the Hilbert transform has been termed the Hilbert-Huang Transform (HHT).

Given a signal $x(t)$, the EMD algorithm seeks for its characteristic time scales, which are defined by the time lapse between successive extrema [8]. A systematic means of extracting the different time scales, designated the sifting process, is as follows: (i) identify all local extrema; (ii) interpolate the maxima and the minima by spline approximations to produce the upper and lower envelopes, respectively; (iii) compute $m(t)$, the mean of the upper and lower envelopes; (iv) compute $h(t) = x(t) - m(t)$; (v) if $h(t)$ is not an IMF, restart the procedure by treating $h(t)$ as the signal.

The component $h(t)$ is considered to be an IMF when the mean $m(t)$ is *globally* smaller than a prescribed fraction of the mode amplitude, defined as half the difference of the upper and lower envelopes. Because overiterating for better local approximation may be detrimental to the main portions of the signal, larger values of $m(t)$ may be tolerated locally, as proposed by Rilling et al. [24].

Once the first IMF $h_1(t)$ has been computed, the second IMF can be extracted from the residue $r_1(t) = x(t) - h_1(t)$. By construction, the number of extrema in the residue decreases with the number of IMFs,

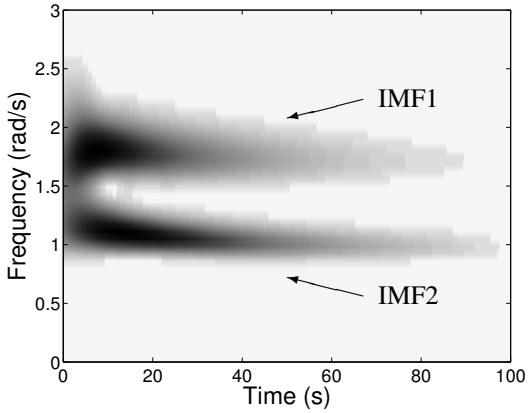

Figure 2: Wavelet transform applied to signal $y(t)$ in Figure 1(b).

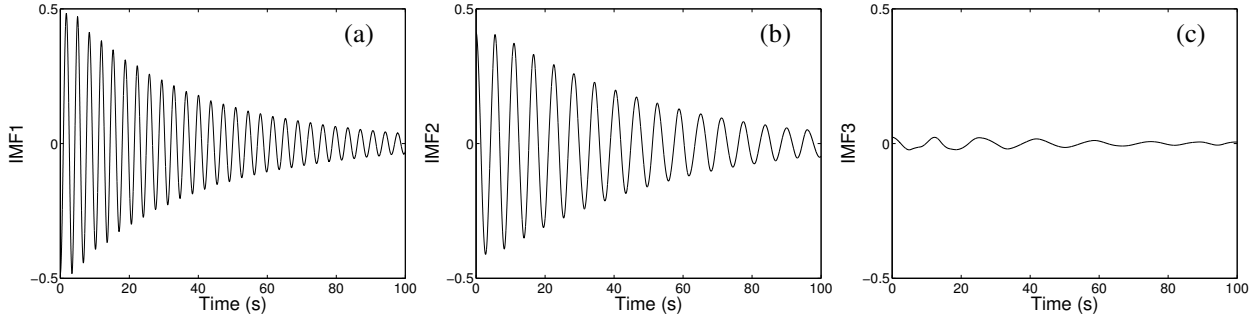

Figure 3: Application of the EMD to signal $y(t)$ in Figure 1(b). (a) First IMF; (b) second IMF; (c) third IMF.

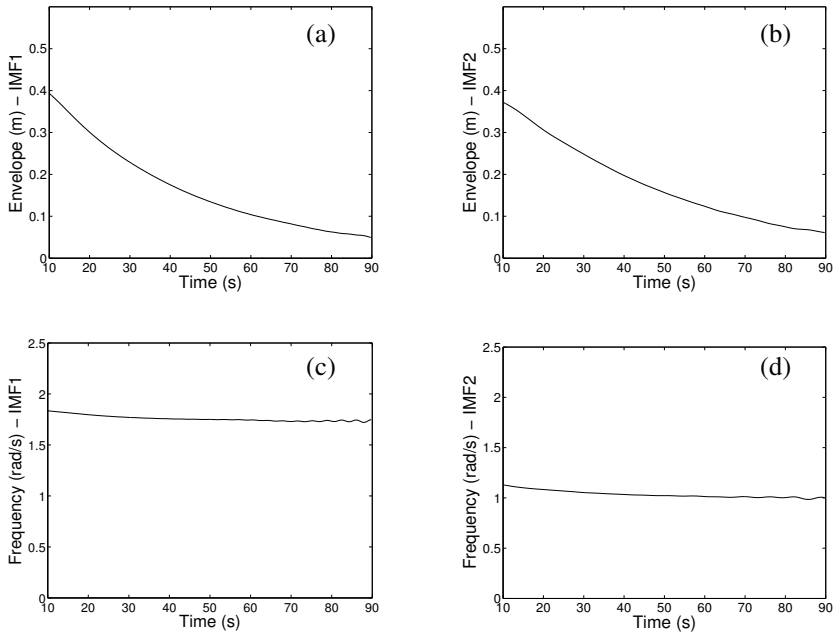

Figure 4: Final outcome of the HHT applied to a two-component signal. (a) Envelope of the first IMF; (b) envelope of the second IMF; (c) instantaneous frequency of the first IMF; (d) instantaneous frequency of the second IMF

and the iterative process stops when the residue after n iterations $r_n(t)$ becomes a monotonic function. By summing up all the IMFs and the last residue, the complete signal decomposition is obtained:

$$x(t) = \sum_{k=1}^{n} h_k(t) + r_n(t). \tag{11}$$

Because the EMD explores sequentially the different time scales in the data, going from the finest scale (i.e., the highest-frequency component) to the coarsest scale (i.e., the lowest-frequency component), it is characterized by an inherent multiresolution.

For illustration, the multicomponent signal $y(t)$ in Figure 1(b) is considered. Figure 2 depicts the wavelet transform of this signal, which reveals the presence of two dominant frequency components in the vicinity of the natural frequencies of the linearized system. The application of the HHT begins with the decomposition of the signal in terms of its IMFs using EMD. The 3 leading IMFs are displayed in Figure 3. The first 2 IMFs are related to the fundamental frequency components and account for more than 99.5% of the total variance in the signal, which confirms that $y(t)$ can be approximated using a two-component signal. The last IMF can be physically interpreted by considering its harmonic content; in particular, its characteristic frequency is equal to 2 times that of the second IMF minus that of the first IMF. This is remarkable, because this component was completely missed by the wavelet transform. The Hilbert transform can now be safely applied to each of the IMFs. The final outcome of the HHT in terms of amplitude and instantaneous frequency of the first two IMFs is shown in Figure 4. The respective contributions of the modes can be easily assessed from Figures 4(a) and (b); that is, both modes seem to participate evenly in the system response. Moreover, because the instantaneous frequencies of both modes decrease with time, the hardening effect of the nonlinearity is evident in Figures 4(c) and (d). Clearly, this represents meaningful structural information, which cannot be obtained from the visual inspection of the time series.

In summary, the HHT represents an important addition to the structural dynamicist's signal processing toolbox. What makes the HHT so attractive is that it eliminates the need for an a priori defined functional basis, as is generally required for traditional signal analysis techniques (e.g., the Fourier transform expresses a signal in terms of global harmonic basis functions, and the wavelet transform in terms of local basis functions). Being purely data-driven, the HHT precisely determines the most appropriate empirical but adaptive basis. This ability to adapt is crucial, given the individualistic nature of nonlinear systems. Another key feature of the method is that, by utilizing the Hilbert transform, it operates at the scale of one oscillation and is, thus, truly able to track local changes in signals.

4 The Intimate Relation between the CxA Method and the HHT

The proposed nonlinear system identification technique, termed the slow-flow model identification (SFMI) method, integrates elements of the previously discussed CxA process and the HHT-based slow-flow reduction of the dynamics. Before we proceed to describe the detailed tasks that need to be undertaken in order to develop and test the SFMI method, it is necessary to establish a relationship between the theoretical CxA approach and the computational HHT method. The missing link between these two seemingly distinct approaches was first revealed in [18].

Both approaches share a common basis by expanding a multifrequency signal in terms of a series of simple, monocomponent oscillatory modes, which are related to the dominant fast-frequency components of the signal. On the one hand, the CxA method transforms the equations of motion of a nonlinear system into a set of approximate equations that govern the slow flow. Two equations, one for the amplitude and one for the phase, are derived for each modeled fast-frequency component, governing the slow modulation of that fast harmonic. On the other hand, the HHT characterizes a signal through the amplitude and phase of the elemental oscillatory components, the IMFs.

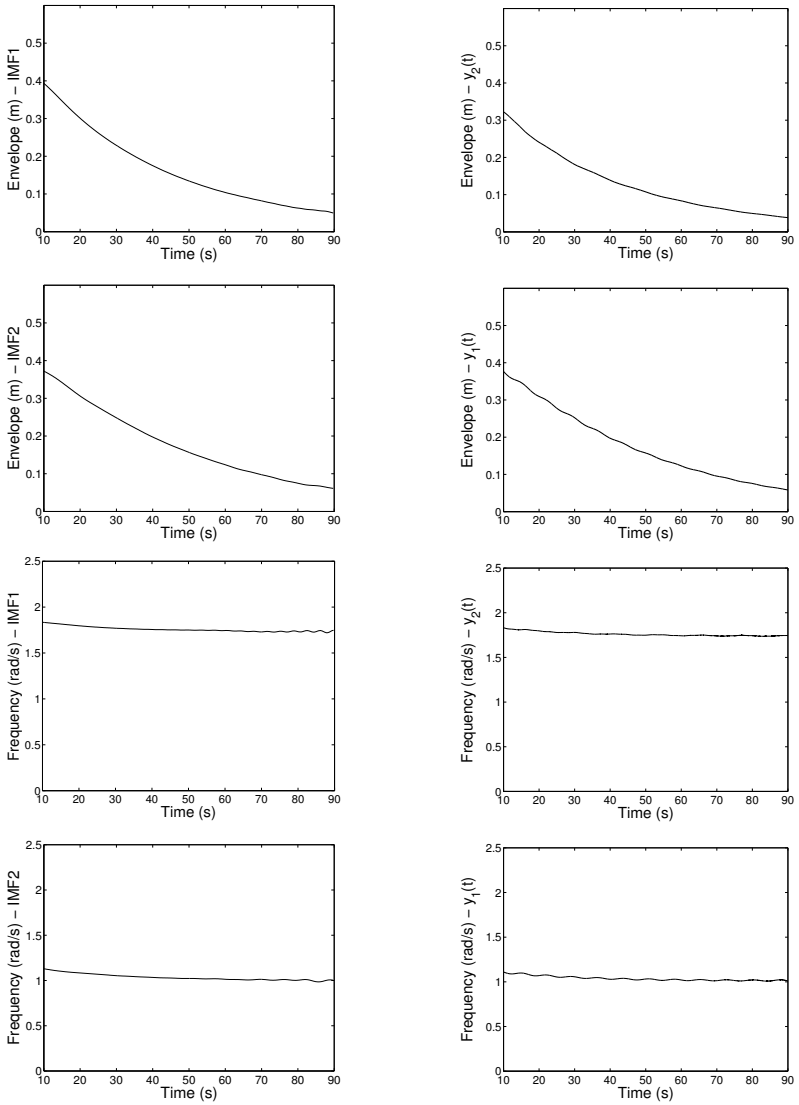

Figure 5: Intimate relation between the theoretical CxA approach and the computational HHT method. Left column: HHT results; right column: CxA results.

Hence, the link between the methods is clear: *the slow-flow model derived using the CxA method corresponds to the equations governing the amplitude and phase of the dominant IMFs computed from the signal by applying the HHT; the CxA method therefore provides a rigorous theoretical framework for the HHT*.

To illustrate the relation between both approaches, Figure 5 shows the comparison of the results of the CxA and HHT methods applied to the response $y(t)$ of system (8) with $k_1 = k_2 = k_{12} = m_1 = m_2 = 1$, $k_{nl} = 2$, $c_1 = c_2 = 0.05$, $c_{12} = 0$ and zero initial conditions except for $x(0) = 1$. The four top plots depict the temporal evolution of the envelopes of the modeled components in the CxA method, $y_1(t)$ and $y_2(t)$, and of the IMFs, respectively. The four bottom plots depict the temporal evolution of the corresponding instantaneous frequencies. An almost complete coincidence of the two sets of results is observed, confirming the link between the two methods.

Based on this theoretical link, the SFMI method is formulated with the following steps:

1. Perform experimental measurements of the transient response of the tested system to obtain a set of local time series at different sensing positions throughout the system.
2. Analyze each individual time series using the wavelet transform to identify the dominant frequency components and their temporal evolution.
3. Apply the HHT to the measured time series.

4. By comparing the wavelet spectrum to the individual plots of the instantaneous frequencies of the extracted IMFs, determine the dominant IMFs of the structural response and categorize them in terms of their characteristic time scales.
5. Based on the slow-flow model of the CxA method, perform a curve-fitting of the measured instantaneous frequencies and amplitudes of the IMFs using a classical linear least-squares procedure; doing so, the physical parameters are identified.
6. Assess the accuracy of the identification process by comparing the measured and reconstructed time series.

One key feature of the SFMI method is that it performs a multiscaled identification, because it employs the characteristic time scales of the dominant dynamics at different phases (time windows) of the system response at different sensing locations.

5 The Slow-Flow Model Identification Method: Numerical Results

To demonstrate the effectiveness of the SFMI method for characterization and parameter estimation of MDOF nonlinear systems, the identification of the 2DOF system (8) is considered. Its slow-flow model can be recast in matrix form

$$\overbrace{\begin{bmatrix} -\frac{a_3\sin(\beta_3-\beta_1)}{2\omega_1} & 0 & 0 & 0 & \frac{a_1}{2} & 0 & \frac{a_1-a_3\cos(\beta_3-\beta_1)}{2} \\ -\frac{a_4\sin(\beta_4-\beta_2)}{2\omega_2} & 0 & 0 & 0 & \frac{a_2}{2} & 0 & \frac{a_2-a_4\cos(\beta_4-\beta_2)}{2} \\ -\frac{a_1\sin(\beta_1-\beta_3)}{2\omega_1} & 0 & 0 & 0 & 0 & \frac{a_2}{2} & \frac{a_3-a_1\cos(\beta_1-\beta_3)}{2} \\ -\frac{a_2\sin(\beta_2-\beta_4)}{2\omega_2} & 0 & 0 & 0 & 0 & \frac{a_2}{2} & \frac{a_4-a_2\cos(\beta_2-\beta_4)}{2} \\ \frac{a_3\cos(\beta_3-\beta_1)-a_1}{a_1} & -1 & 0 & 0 & 0 & 0 & \frac{-a_3\omega_1\sin(\beta_3-\beta_1)}{a_1} \\ \frac{a_4\cos(\beta_4-\beta_2)-a_2}{a_2} & -1 & 0 & 0 & 0 & 0 & \frac{-a_4\omega_2\sin(\beta_4-\beta_2)}{a_2} \\ \frac{a_1\cos(\beta_1-\beta_3)-a_3}{a_3} & 0 & -1 & -\frac{3a_3^2}{4\omega_1^2}-\frac{3a_4^2}{2\omega_2^2} & 0 & 0 & \frac{-a_1\omega_1\sin(\beta_1-\beta_3)}{a_3} \\ \frac{a_2\cos(\beta_2-\beta_4)-a_4}{a_4} & 0 & -1 & -\frac{3a_4^2}{4\omega_2^2}-\frac{3a_3^2}{2\omega_1^2} & 0 & 0 & \frac{-a_2\omega_2\sin(\beta_2-\beta_4)}{a_4} \end{bmatrix}}^{\mathbf{A}} \overbrace{\begin{bmatrix} k \\ k_1 \\ k_2 \\ k_{nl} \\ c_1 \\ c_2 \\ c_{12} \end{bmatrix}}^{\mathbf{x}} = -\overbrace{\begin{bmatrix} m_1\dot{a}_1 \\ m_1\dot{a}_2 \\ m_2\dot{a}_3 \\ m_2\dot{a}_4 \\ m_1(2\omega_1\dot{\beta}_1+\omega_1^2) \\ m_1(2\omega_2\dot{\beta}_2+\omega_2^2) \\ m_2(2\omega_1\dot{\beta}_3+\omega_1^2) \\ m_2(2\omega_2\dot{\beta}_4+\omega_2^2) \end{bmatrix}}^{\mathbf{b}} \tag{12}$$

An estimation of the matrix $\mathbf{A}$ and the vector $\mathbf{b}$ can be obtained by direct application of the HHT, through the computation of the envelopes a_i and phases β_i (and their first derivatives) of the measured IMFs. We note that, if the mass matrix is unknown, the identified coefficients are therefore mass-normalized.

A careful inspection of equation (12) reveals that the elements of matrix $\mathbf{A}$ involving the term $\sin(\beta_i - \beta_j)$ must be very small, which might corrupt the curve-fitting process. The reason is that the phase differences $(\beta_3 - \beta_1)$, $(\beta_2 - \beta_4)$, $(\beta_1 - \beta_3)$ and $(\beta_2 - \beta_4)$ should be very close to 0 or $\pm\pi$, because they correspond to either the in-phase or anti-phase mode. The slow-flow model can therefore be rewritten by removing those elements from matrix $\mathbf{A}$, and the physical parameters contained in vector $\mathbf{x}$ can be identified in a straightforward manner using the Moore-Penrose inverse

$$\mathbf{x} = (\mathbf{A}^T\mathbf{A})^{-1}\mathbf{A}^T\mathbf{b} \tag{13}$$

The response of system (8) is computed using Newmark's algorithm for $k_1 = k_2 = k_{12} = m_1 = m_2 = 1$, $k_{nl} = 2$, $c_1 = c_2 = 0.05$, $c_{12} = 0$ and two sets of initial conditions, $x(0) = 0.5$ and $x(0) = 1$, and all other initial conditions set to zero. Because the extrema of the transient responses must be correctly identified in the EMD, a fair number of data points per oscillation is required. In the present study, the sampling frequency is set to 10 Hz. The system response for $x(0) = 1$ is displayed in Figure 1.

Parameter estimation is carried out using the SFMI method, and the results are listed in Table 1, respectively. A satisfactory identification of the stiffness and damping parameters is realized. The remaining small errors are attributed to the inherent approximations of the CxA process.

	k_1 (N/m)	k_2 (N/m)	k (N/m)	k_{nl} (N/m^3)	c_1 (Ns/m)	c_2 (Ns/m)	c_{12} (Ns/m)
Exact values	1	1	1	2	0.05	0.05	0
Identification $x(0) = 0.5$	0.995	0.983	1.000	2.143	0.044	0.047	0.003
Identification $x(0) = 1$	1.001	0.976	1.006	2.107	0.047	0.048	0.001

Table 1: Parameter estimation results for system (8).

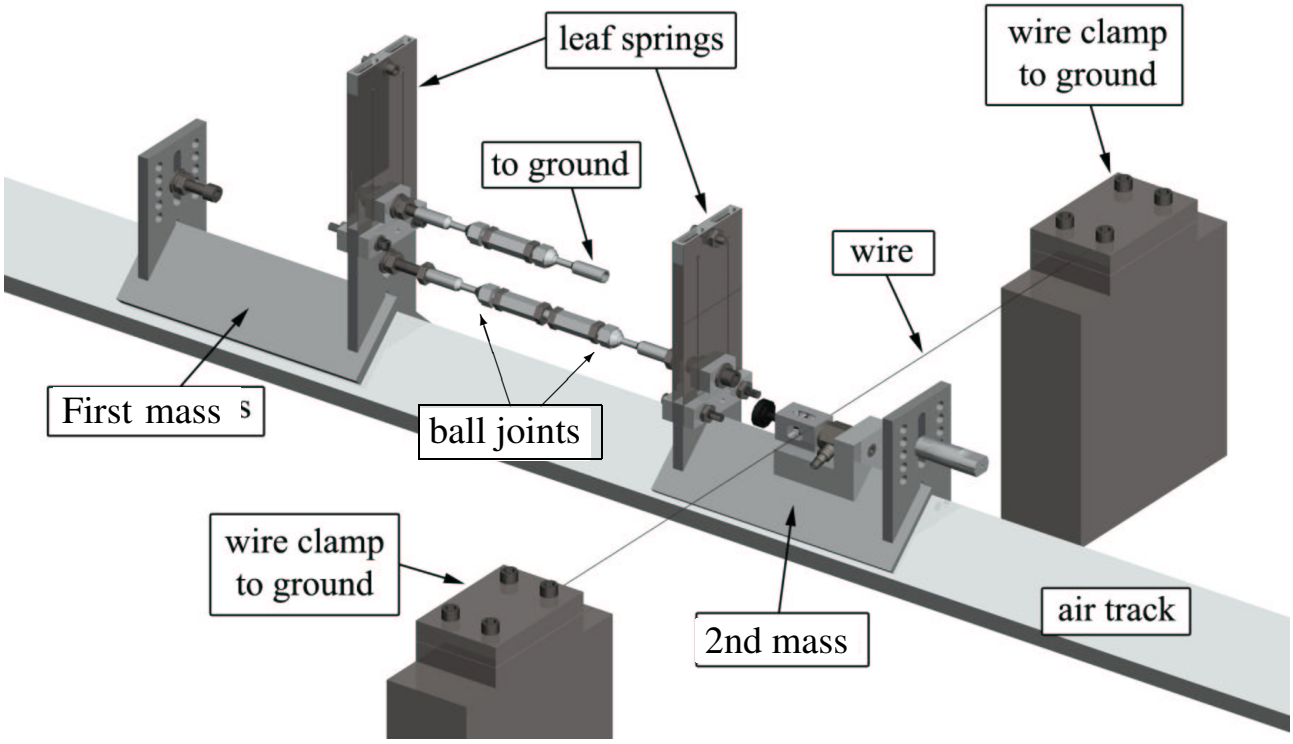

Figure 6: Schematic of the experimental fixture.

6 The Slow-Flow Model Identification Method: Experimental Demonstration

6.1 Description of the experimental fixture

To support the previous theoretical findings, experimental measurements were carried out using the fixture depicted in Figure 6. This fixture realized the system described by equations

$$\begin{aligned} m_1\ddot{x} + c_1\dot{x} + c_{12}(\dot{x} - \dot{y}) + k_1 x + k_{12}(x - y) &= 0 \\ m_2\ddot{y} + c_{12}(\dot{y} - \dot{x}) + c_2\dot{y} + k_{12}(y - x) + k_{nl}y^3 &= 0 \end{aligned} \tag{14}$$

and comprised two cars made of aluminum angle stock which were supported on a straight air track. The first car (i.e, the left car in the upper picture in Figure 6) of mass m_1 was grounded by means of a linear spring k_1, and the second car of mass m_2 was connected to the first car by means of a linear coupling stiffness k_{12}. The leaf springs k_1 and k_{12} were built to be identical. An essential cubic nonlinearity k_{nl} was realized by a thin wire with no pretension, as detailed in [25]. A long-stroke electrodynamic shaker was used to excite the first car.

The response of both oscillators was measured using accelerometers. Estimates of the corresponding displacements were obtained by integrating twice the measured accelerations. The resulting signals were then

Parameter	Value
Stiffness k_1	427.2 N/m
Coupling stiffness, k_{12}	421.1 N/m
Cubic stiffness k_{nl}	$5.77\,10^6$ N/m^3
Damping c_1	0.13 Ns/m
Damping c_2	0.05 Ns/m

Table 2: Parameters of the experimental fixture identified using the stochastic subspace identification and restoring force surface methods.

Parameter	Value
Stiffness k_1	447.3 N/m
Coupling stiffness, k_{12}	402.9 N/m
Stiffness k_2	4.4 N/m
Cubic stiffness k_{nl}	$6.15\,10^6$ N/m^3
Damping c_1	0.39 Ns/m
Damping c_2	0.35 Ns/m
Damping c_{12}	0.01 Ns/m

Table 3: Parameters of the experimental fixture identified using the SFMI method.

high-pass filtered to remove the spurious components introduced by the integration procedure.

6.2 Separate identification of the system components

Before treating the system of coupled cars using the SFMI method, a separate identification of the different components was carried out:

- The first car was disconnected from the second car, and linear modal analysis was performed on the disconnected first car using the stochastic subspace identification technique [26]. The natural frequency and the viscous damping ratio were estimated to be 4.49 Hz and 0.42%, respectively. Because the mass of the first car was known, the stiffness and damping parameters k_1 and c_1 were easily deduced from this modal analysis. A similar procedure was undertaken to estimate coefficient k_{12}.
- The second car was disconnected from the first car with the aim of estimating the nonlinear coefficient k_{nl}. To this end, the restoring force surface method [3] was employed. Further details are available in [22].

The values of the parameters identified using this two-step procedure are listed in Table 2.

Finally, the wire was disconnected, and a modal analysis of the coupled linear system was performed. The natural frequencies predicted by the previously identified parameters overestimated the measured ones by 3%. To get a better match between measured and predicted frequencies, the estimate of the coupling stiffness k_{12} was decreased to 395 N/m. Rigorously, however, one should introduce a detailed modeling of the connection between the two cars which comprises ball joints (see Figure 6).

6.3 Nonlinear system identification using the SFMI method

The identification of the coupled nonlinear system is now undertaken using the 6-step procedure introduced in Section 4.

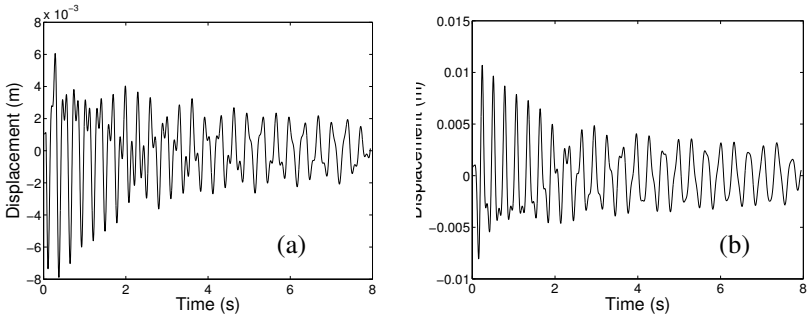

Figure 7: Measured displacement signals. (a) First car; (b) second car.

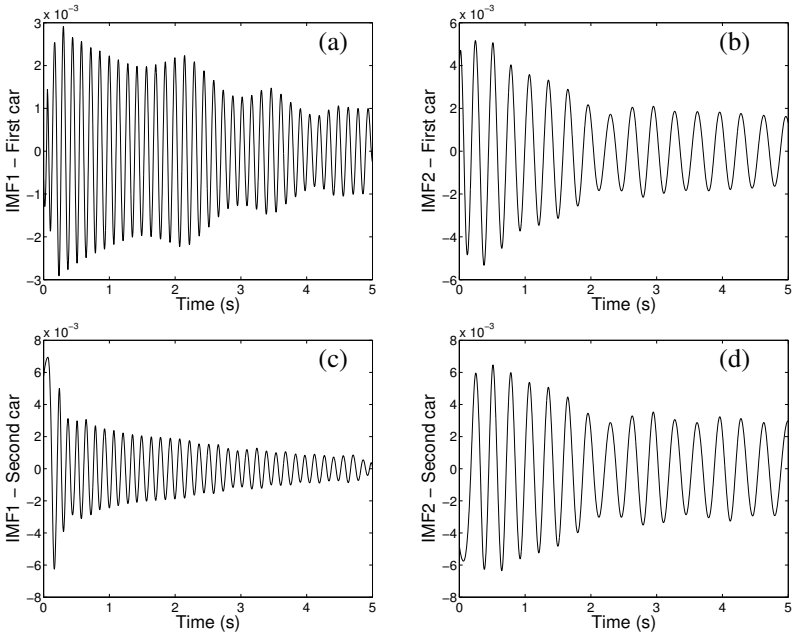

Figure 8: EMD applied to the measured displacements. (a,b) First car; (c,d) second car

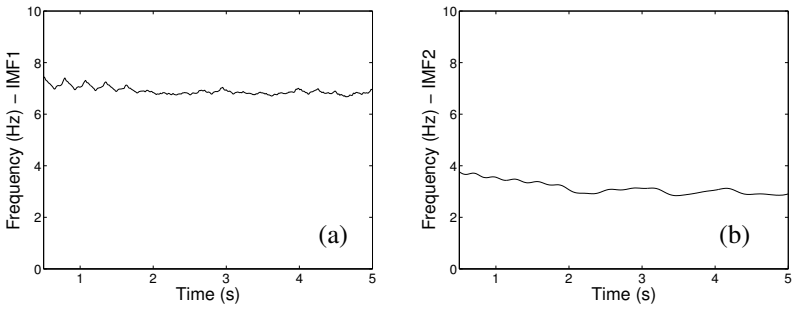

Figure 9: Measured instantaneous frequencies of the first car. (a) First IMF; (b) second IMF.

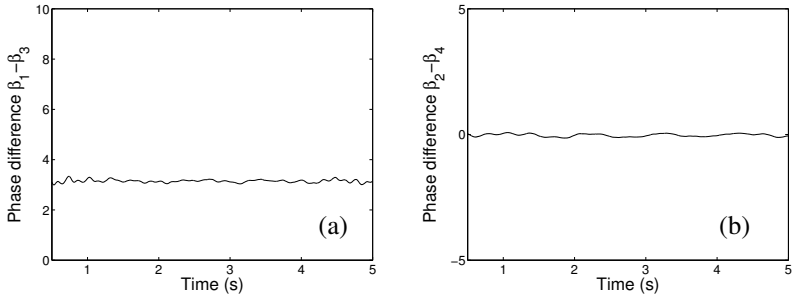

Figure 10: Measured phase differences. (a) Anti-phase mode: $\beta_1 - \beta_3$; (b) in-phase mode: $\beta_2 - \beta_4$.

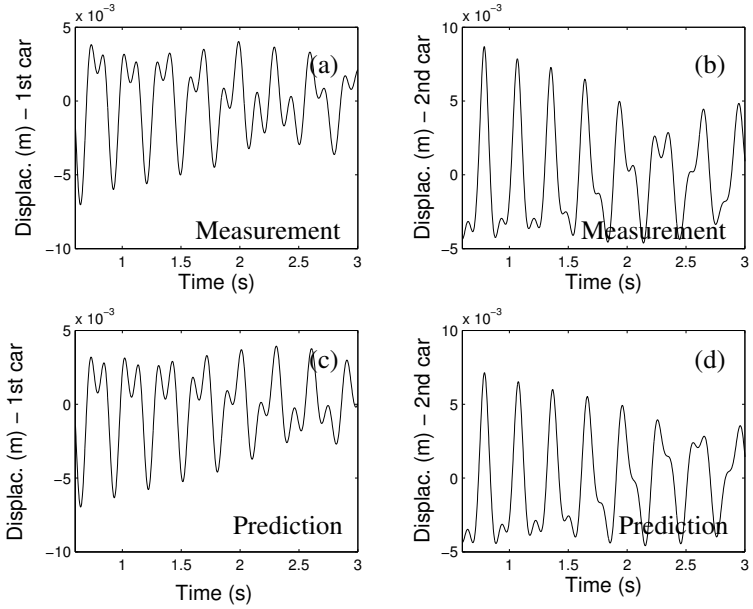

Figure 11: Comparison of the predicted and measured displacements. (a,c) First car; (b,d) second car.

The displacement signals computed from the measured accelerations are depicted in Figure 7; the participation of both the in-phase and anti-phase modes in the system response is evident. The wavelet transform (not depicted herein) shows two dominant frequency components in the vicinity of the natural frequencies of the underlying linear system. Processing the measured displacements through the EMD, one obtains the dominant IMFs in Figure 8. The 2 leading IMFs account for 99.8 and 99.9% of the total variance of the displacement of the first and second cars, respectively. The Hilbert transform is then applied sequentially to each identified IMF. Figure 9 depicts the instantaneous frequencies of the IMFs of the first car. The frequency of the in-phase mode decreases from 3.8 Hz at $t = 0.5\,s$ to 2.9 Hz at $t = 5\,s$, which is an indication of a strongly nonlinear system. We note that, due to the end effects of the EMD and the Hilbert transform, the first half second of data is systematically discarded in what follows.

The next step in the nonlinear system identification process is the estimation of the system parameters [1]. We note that the measured phase differences $\beta_1 - \beta_3$ and $\beta_2 - \beta_4$ in Figure 10 are close to π and 0. Table 3 summarizes the results of the linear least-squares fitting, and the resulting parameters can be compared to those obtained from the separate identification of the system components:

- The identified stiffnesses k_1 and k_{12} differ from the values in Table 2 by a few percent. As discussed in the previous section, a decrease in the value of k_{12} was expected due to the presence of ball joints in the connection between the two cars.

[1] Prior to system identification, both cars were weighed. Their masses were found to be $m_1 = 0.632\,\text{kg}$ and $m_2 = 0.558\,\text{kg}$.

- The nonlinear coefficient is in close agreement with the value previously identified. Moreover, because k_2 takes a very small value, the SFMI method is able to retrieve that the nonlinearity is essential; that is there is no linear spring in parallel with the nonlinear spring.
- Estimated damping is somewhat higher compared to that in Table 2.

The predicted and measured displacements are compared in Figure 11, which highlights the predictive capability of the identified model.

The SFMI method was also tested in [22] for another impulsive force with an amplitude reduced by 30%. Despite some slight discrepancies, the identified parameters agree well with those in Table 3.

Because a strongly nonlinear system is investigated and because damping estimation is a difficult problem in this fixture, all these results can be considered as satisfactory and demonstrate the effectiveness of the SFMI method.

7 Concluding Remarks

This paper focuses on the relation between the theoretical CxA approach and the computational HHT with the aim of bringing to light a better understanding of this time-frequency transform and developing a new nonlinear system identification approach of rather general applicability in nonlinear structural dynamics. A one-to-one relationship between the analytically realized slow-flow dynamics of the system and the IMFs derived directly from the measured time series is demonstrated. Based on the theoretical link between the two approaches, the SFMI method is proposed. This method has several interesting features:

- Because it is based on the HHT, the SFMI method fully embraces both the nonlinearity and nonstationarity of operating dynamical systems. Moreover, a multiscaled identification is performed, because the method identifies the dominant characteristic time scales of the system response and establishes the dimensionality of the dominant dynamics.
- The Hilbert transform gives sharper frequency and time resolutions compared to other time-frequency decompositions. Another distinct advantage is that ridge extraction, which is necessary when using the wavelet and Gabor transforms for nonlinear system identification is avoided.
- Due to its specific time-frequency representation, the SFMI method certainly offers a different perspective on the dynamics. For instance, the computation (and subsequent comparison) of the instantaneous frequencies of the IMFs can reveal possible nonlinear resonant interactions between the system's components that might be embedded and, thus, hidden in the signal [27].
- The SFMI method is a 'linear-in-the-parameters' method and does not rely on nonlinear optimization techniques, which greatly facilitates parameter estimation.

Mode mixing may potentially be an issue when using the HHT, especially in the case of noisy data and signals with substantially different modal participations. Use of the HHT intermittency test or appropriate filtering should resolve this difficulty. The fact that the slow-flow model of the dominant dynamics computed through the CxA approach is an approximation of the true dynamics may also be seen as a limitation. However, the predictive accuracy of the slow-flow model can be as good as desired by including the necessary number of harmonic components in the ansatz.

In summary, the numerical and experimental application examples in this study show that the SFMI method yields quite accurate results and offers an effective tool for parameter estimation of MDOF nonlinear dynamical structures.

Acknowledgments

G. Kerschen is supported by a grant from the Belgian National Fund for Scientific Research (FNRS) which is gratefully acknowledged.

The authors are grateful to Patrick Flandrin for making his EMD code freely available at http://perso.ens-lyon.fr/patrick.flandrin (see also [24]).

References

[1] Worden, K. and Tomlinson, G.R., 2001, Nonlinearity in Structural Dynamics: Detection, Identification and Modelling, Institute of Physics Publishing, Bristol, Philadelphia.

[2] Kerschen, G., Worden, K., Vakakis, A.F. and Golinval, J.C., 2006, "Past, present and future of nonlinear system identification in structural dynamics," Mechanical Systems and Signal Processing 20, 505-592.

[3] Masri, S.F. and Caughey, T.K., 1979, "A nonparametric identification technique for nonlinear dynamic problems," Journal of Applied Mechanics 46, 433-44.

[4] Feldman, M., 1994, "Nonlinear system vibration analysis using the Hilbert transform - I. Free vibration analysis method FREEVIB," Mechanical Systems and Signal Processing 8, 119-127.

[5] Feldman, M., 1997, "Non-linear free vibration identification via the Hilbert transform," Journal of Sound and Vibration 208, 475-489.

[6] Garibaldi, L., Ruzzene, M., Fasana, A. and Piombo, B., 1998, "Identification of non-linear damping mechanisms using the wavelet transform," Mecanique Industrielle et Materiaux 51, 92-94.

[7] Bellizzi, S., Gullemain, P. and Kronland-Martinet, R., 2001, "Identification of coupled non-linear modes from free vibration using time-frequency representation," Journal of Sound and Vibration 243, 191-213.

[8] Huang, N.E., Shen, Z., Long, S.R., Wu, M.C., Shih, H.H., Zheng, Q., Yen, N.C., Tung, C.C. and Liu, H.H., 1998, "The empirical mode decomposition and the Hilbert spectrum for nonlinear and non-stationary time series analysis," Proceedings of the Royal Society of London, Series A — Mathematical, Physical and Engineering Sciences 454, 903-995.

[9] Kakurin, A.M and Orlovsky, I.I., 2005, "Hilbert-Huang transform in MHD plasma diagnostics," Plasma Physics Reports 31, 1054-1063.

[10] Huang, N.E., Wu M.L., Qu W.D., Long, S.R. and Shen, S.S.P., 2003, "Applications of Hilbert-Huang transform to non-stationary financial time series analysis," Applied Stochastic Models in Business and Industry 19, 245-268.

[11] Huang, N.E., Wu M.L., Qu W.D., Long, S.R. and Shen, S.S.P., Editors, 2003, Hilbert-Huang Transform and Its Applications, World Scientific, Singapore.

[12] Yang, J.N., Lei, Y., Lin, S. and Huang, N., 2004, "Hilbert-Huang based approach for structural damage detection", Journal of Engineering Mechanics 130, 85-95.

[13] Yu, D., Cheng, J. and Yang, Y., 2005, "Application of EMD method and Hilbert spectrum to the fault diagnosis of roller bearings," Mechanical Systems and Signal Processing 19, 259270.

[14] Brenner, M. and Prazenica, C., 2005, "Aeroelastic flight data analysis with the Hilbert-Huang algorithm," AIAA Atmospheric Flight Mechanics Conference and Exhibit, San Francisco, 2005-5917.

[15] Pai, F.P. and Hu, J., 2006, "Nonlinear vibration characterization by signal decomposition," Proceedings of the 24th International Modal Analysis Conference (IMAC), St. Louis.

[16] Yang, J.N., Lei, Y., Pan, S.W. and Huang, N., 2003, "System identification of linear structures based on Hilbert-Huang spectral analysis; Part 1: Normal modes," Earthquake Engineering and Structural Dynamics 32, 1443-1467.

[17] Yang, J.N., Lei, Y., Pan, S.W. and Huang, N., 2003, "System identification of linear structures based on Hilbert-Huang spectral analysis; Part 2: Complex modes," Earthquake Engineering and Structural Dynamics 32, 1533-1554.

[18] Kerschen, G., Vakakis, A.F., Lee, Y.S., McFarland, D.M. and Bergman, L.A., 2006, "Toward a fundamental understanding of the Hilbert-Huang Transform in nonlinear structural dynamics," Proceedings of the 24th International Modal Analysis Conference (IMAC), St-Louis.

[19] Sanders, J.A. and Verhulst, F., 1985, Averaging Methods in Nonlinear Dynamics Systems, Springer-Verlag, New York.

[20] Manevitch, L.I., Complex representation of dynamics of coupled oscillators in Mathematical Models of Nonlinear Excitations, Transfer Dynamics and Control in Condensed Systems, New York, Kluwer Academic/Plenum Publishers, pp. 269-300, 1999.

[21] Lochak, P. and Meunier, C., 1988, Multiphase Averaging for Classical Systems with Applications to Adiabatic Theorems, Springer Verlag, Berlin and New York.

[22] Kerschen, G., Vakakis, A.F., Lee, Y.S., McFarland, D.M. and Bergman, L.A., Toward a Fundamental Understanding of the Hilbert-Huang Transform in Nonlinear Dynamics, Journal of Vibration and Control, in review.

[23] Kerschen, G., Lee, Y.S., Vakakis, A.F., McFarland, D.M. and Bergman, L.A., 2006, "Irreversible passive energy transfer in coupled oscillators with essential nonlinearity," SIAM Journal on Applied Mathematics 66, 648-679.

[24] Rilling, G., Flandrin, P. and Goncalves, P., 2003, "On empirical mode decomposition and its algorithms," IEEE-EURASIP Workshop on Nonlinear Signal and Image Processing NSIP-03, Grado.

[25] McFarland, D.M., Bergman, L.A. and Vakakis, A.F., 2005, "Experimental study of non-linear energy pumping occurring at a single fast frequency," International Journal of Non-linear Mechanics 40, 891-899.

[26] Van Overschee, P. and DeMoor, B., 1996, Subspace Identification for Linear Systems: Theory, Implementation, Applications, Kluwer Academic Publishers, Boston.

[27] Georgiades, F., Vakakis, A.F. and Kerschen, G., 2006, "Broadband irreversible targeted energy transfer from a linear dispersive rod to a lightweight essentially nonlinear end attachment," International Journal of Non-linear Mechanics, in press.